ENHANCING AG MILLING CIRCUIT PERFORMANCE THROUGH ADVANCED LINER DESIGN, MODELLING, MATERIAL SELECTION AND DIGITAL TOOLS

Wei Chen[1, 2], *Matt Hazell[1], Christian Moreno[1], Gabe Larose[1], Craig Faulkner[1]

[1]Bradken Inc
90 Richmond Street E Suite 400, Toronto, Ontario, M5C 1P1 Canada
(*Corresponding author: mhazell@bradken.com)

[2]School of Intelligent Manufacturing, Xi'an Jiaotong-Liverpool University
Suzhou Industrial Park, Suzhou, Jiangsu, P. R. China 215123

Abstract

Liner design and its material selection are of critical value to the performance of the autogenous grinding mill and its associated circuit. This study utilised advanced liner design methodology to develop a full AG mill liner package with focus on the shell and discharge end to generate and discharge the product stream. Balance between the AG milling and pebble crushing was also modelled with advanced numerical modelling tools to reduce the overall circuit specific energy. Strategic selection of liner material for grates was used to mitigate risk of major design revisions and provide performance validation in service before revising to align with reline and increased overall reliability needs. A suite of digital tools was developed and utilised to track, report and construct a machine learning model for long-term production forecasting purpose. Results yielded over 9.5% increase of AG mill throughput and 2.5% reduction of the overall circuit specific energy. The machine learning model constructed from the historical campaign data also showed high accuracy in predicting upcoming circuit performance. The outcome of this study has significantly increased the production performance and reliability of the AG milling circuit; as well as, long-term forecasting capability.

Keywords

AG Mill, Advanced Mill Liner Design, Circuit Optimisation

Introduction

Bradken's partner site was a major copper ore operation located in North America. The mill explored in this study was a 32-ft x 13-ft AG mill driven by a fixed speed motor at 76% critical speed. The mill operated bi-directionally with traditional bi-directional radial pulp lifters and top-hat high-low shell liners. The lining system were high-chrome alloy with a total of 450 liners per set and a total mass calculated at 312,404 kgs. The mill utilised a 7-axis 2500kg Russell reline machine. The mill was inspected regularly with planned stoppage and inspection at 42 day intervals. The mill operated at an average throughput of 814tph across a typical liner campaign.

In 2019, site explored an expansion project that would increase site production by 20ktpd. While several options were considered, including the conversion of mills to SAG operation, it was ultimate decided to increasing pebble crusher capacity. To maximise this available capacity, the upstream AG mills were required to increase production.

This article outlines the design approach and optimisation completed to accomplish sites target objective. This includes advanced liner design initiatives supported by numerical modeling and the digital tools used to successfully forecast and guarantee those results.

Method

This project was executed following a solution focused collaborative approach where all major stakeholders were commissioned to provide equitable contribution to the discussion. A team was organised to include the primary contributors from each party to achieve the target outcome of increasing the partner sites AG mill discharge production.

- Site: Management, metallurgists, operations.
- Corporate Owner: Operational improvement, corporate metallurgist.
- Bradken: Sales, regional design engineering, principle process engineer.

The optimisation of components followed an iterative revisionist approach. Concepts were generated through collaborative discussion across the assembled team leveraging sites experience and supported by Bradken's global experience and simulation capabilities. Designs were examined through numerical modelling for quantitative comparative justification. Parts were then manufactured and installed for continuous monitoring and validation in service. Practical results were compiled post-process and analysed coupled with further numerical modelling to validate and revise design features to improve performance. The revised designs were then implemented with a performance guarantee. The production data was used to generate an ensemble model performance predictor tool used to track and forecast the AG mills service results.

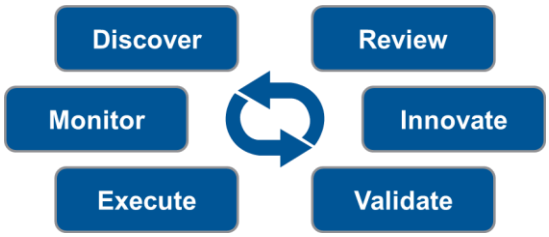

Figure 1: Simplification of Iterative Approach

Discussion

CONCEPT GENERATION AND JUSTIFICATION USING NUMERICAL MODELLING TOOLS

Each region of the mill was examined independently for opportunities to optimise and in consideration of the overall target objective of increasing production. While production increase was the target outcome, revisions to maximise handler capacity and to reduce the number of liner components were also pursued to improve the total cost of ownership. The driving liner design initiative to suit the target objective of increase mill production was to convert the mill to uni-directional operation. This would allow for the implementation of Bradken's Vortex discharge system proven in the industry to facilitate more efficient discharge.

Discharge System Optimisation

Early simulation work on the existing radial design showed potentially ineffective chamber evacuation and opportunity for backflow reclamation. These results suggested that regardless of an increase in chamber intake through a grate optimisation, the discharge system would not evacuate the chambers effective enough to achieve peak performance potential. The proposed Vortex discharge system would facilitate earlier discharge of pulp chambers reducing the opportunity for backflow as proven in practice across Bradken supplied sites globally.

An identified limitation of the Vortex system was its challenges with maximising available open area. The vortex curvature of the lifters would consume potential slot area reducing the available area to maximise grate intake. To overcome this, a unique half-row double wide Vortex discharge system was explored. This removed alternating lifters on the grates and pulp lifters creating a significant increase in chamber volume and available slot surface area.

The open area and grate design were a critical path to maximise available product stream after grinding. The total open area and discharge system determined the overall discharge throughput and backflow inefficiencies into the pulp chambers and mill. A comparative analysis was completed utilising a DEM-SPH coupled numerical framework to examine the discharge performance of the three concepts [**Figure 2**].

Figure 2: Optimised radial design, Vortex design, half-row double wide Vortex design DEM-SPH Simulations

The optimised radial concept was designed to include the maximum possible open area achievable with a radial arrangement as a benchmark.

A measurement plane was used to review the discharge flow rate results exiting the simulated AG mill. This allowed a quantitative comparative analysis of the throughput predictions obtained through the DEM-SPH numerical model [**Figure 3**].

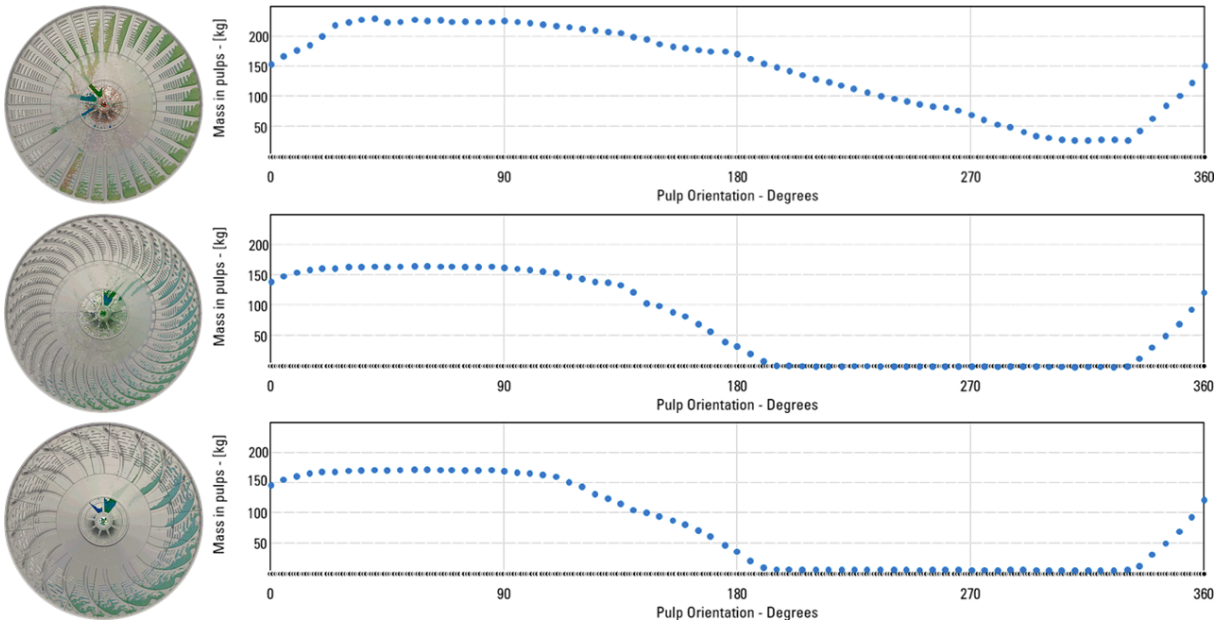

Figure 3: Mass in Pulp Chamber per Rotation [Radial (top), Vortex, Half Row Vortex (bottom)]

The results showed the optimised radial design had significant chamber intake for its geometry, but could not effectively discharge its entire contents, backflowing approximately 11% into the chambers and 9% into the mill. The traditional Vortex efficiently discharged its entire chambers' contents, but left potential opportunity for further discharge if chamber intake could be increased. The half-row Vortex succeeded in maximised chamber intake and also discharging efficiently with a minimal 2% backflow into the chambers.

Effective slot placement was examined through DEM simulation and review. Slot placement was measured against the charge shape and size to ensure they were effectively placed to accept particles into the chamber [**Figure 4**]. Slots were also evaluated against whether they returned particles into the mill during the discharge cycle. This allowed slot placement to be balanced to maximise intake and minimise spill back.

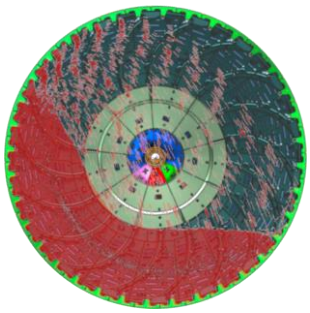

Figure 4: DEM Model Visual Overlay to Examine Slot Charge Capture

While maximising open area, it was imperative to manage both transfer size and throughput. Collaborating with site, the first proposed grate design, REV A, included an increase in overall open area, but a reduced slot size. The desired outcome was to control the product size of the potential increased discharge stream to prevent excess recirculating load. The previous design had a consistent slot size of 3.75in and a total open area of 534in^2

per grate. The REV A design had a top slot size of 3.5in and a small slot size of 2.0in with a total open area of 671.5in^2 per grate.

Risk mitigation became a focus of discussion once the half-row double wide Vortex design was confirmed as the preferred grate. The risks included casting a high-chrome liner with drastic cross-sectional changes across large complex geometry. To mitigate risk, it was agreed with the customer to pursue the first set of Vortex grates in chrome-moly as similar size and complex geometry components had been supplied in this material across the industry. The chrome-moly would have a lower Brinell-hardness than high-chrome typically deployed in SAG operations due to the presence of steel grinding media. Along with the lower Brinell hardness, there was also an expectation of a reduction in wear life compared to the previously supplied high-chrome grates. The chrome-moly liners would be used to validate the designs performance before being revised to meet the wear life.

Bradken undertook a research and development project in parallel to explore casting these liners in high-chrome. An internal study was conducting by Bradken's manufacturing team to simulate the stress, flow, solidification and heat treatment of the castings before pursuing. Once the casting process was verified, trial castings were poured and reviewed with 100% MPI testing. Two trial castings were then supplied to the customer for installation and monitoring in service before scaling to full supply.

Shell Liner Optimisation

A collaborative examination into shell design opportunities was undertaken with the partner site. The initial design proposal targeted opening mill available volume while minimising the deviation from the previously supplied liner design. A combined double wide shell liner was proposed to reduce total mill components and capitalise on available handler capacity. Several factors were considered in the initial proposal including leading face angle and lifter height both of which affect grinding dynamics and wear life performance. A lead face angle was revised from 15° to 5° to promote a high rate of impact grinding [**Figure 5**].

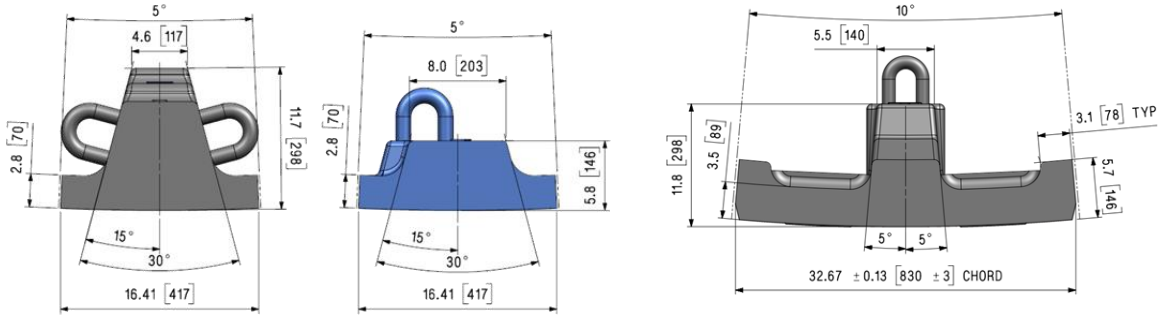

Figure 5: Original Profile Design (left) and Initial Proposed Design (right)

INITIAL IMPLEMENTATION AND MONITORING FOR CONTINUED IMPROVEMENT

After installing the first set of liners, Bradken conducted regular inspections of the mill as part of a continuous wear monitoring program. Scans were taken at each inspection and processed through Bradken's Vision Wear Reporting (VWR) system. The continuous monitoring results were reviewed to validate the installed design in service and identify opportunities for continued development.

The first installed package did not achieve the target mill production, but provided the data required to further optimise the system. Despite the significant increase in total open area, the system did not achieve the desired effect of increasing pulp chamber intake. The reduction in grate top sized slots had an adverse effect on the total mill discharge rate, not just the particle distribution.

POST-PROCESSING NUMERICAL MODELLING ANALYSIS AND REVISION

The site data collected through the initial implementation phase was used in a variety of ways to improve liner design to achieve the required performance. It was also used to build the framework necessary to ensure a performance guarantee.

Discharge System Optimisation

To better normalise variables, it was agreed to revise the grate design to match the slot size and open area of the previous set. This facilitated a more impartial evaluation of the half row pulp chamber system. Bradken also utilised a DEM-SPH coupled numerical framework to examine the transient performance of various open area designs [**Table 1**]. The results showed the half-row double wide Vortex grate with a top sized slot of 3.75in and total open area of 534in^2 outperformed the other revisions with an average discharge rate of 909tph [**Figure 6**].

Table 1: DEM-SPH Modelled Open Area Configurations

Parameter	GL2	Rev A	Rev B Machined	Rev C
Slot Size [in^2]	3.75	2.0/3.5	2.0/3.5	3.75
Open Area per Grate [in^2]	534	671.5	655.5	534
Number of Parts	18	18	18	18
Total Open Area [in^2]	9,619	12, 087	11, 805	9,619

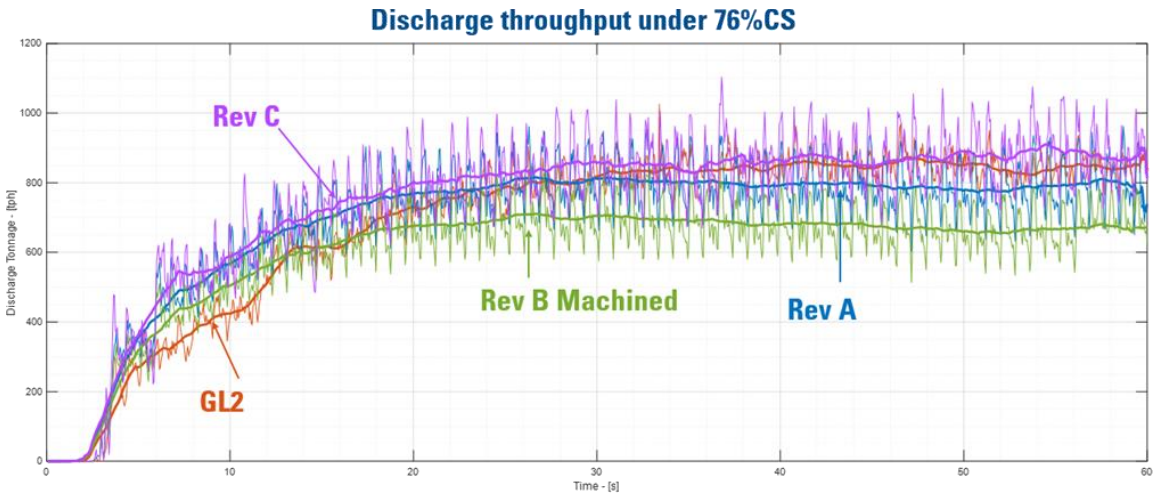

Figure 6: DEM-SPH Results for Various Open Area Configurations

Shell Optimisation

Worn shell profiles were reconstructed from the scan data for DEM modelling and were simulated to evaluate total collision energy results. A probability density function of the collisions results was derived and measured against the recorded mill performance. A distinctive behaviour trend was identified in the total collision energy transitioning from impact to attrition grinding along with liner wear. The data was cross-referenced against

recorded mill performance. A corresponding trend was identified between peak mill production and wear profile that suggested optimal grinding occurred during periods of high attrition grinding and less impact [**Figure 7**]. Utilising the developed collision energy probability approach a revised shell liner design was proposed.

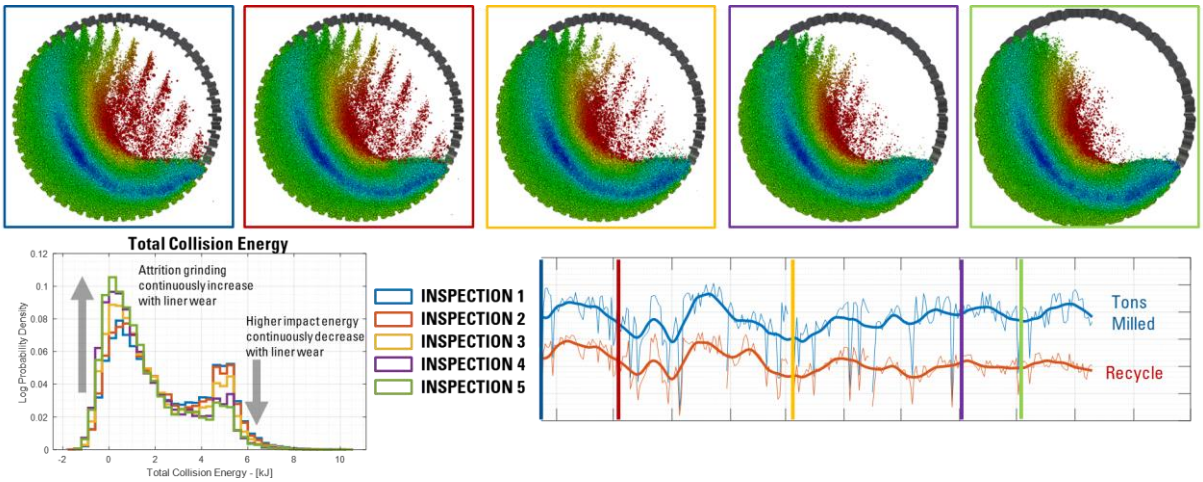

Figure 7: DEM Collision Energy Results Cross-Referenced with Recorded Performance During Service

FINAL REVISION AND RESULTS

Through the preliminary design, initial installation, continued performance monitoring, and post-processing analysis a final revised design was generated with enough data to support the provision of a performance guarantee [**Figure 8**].

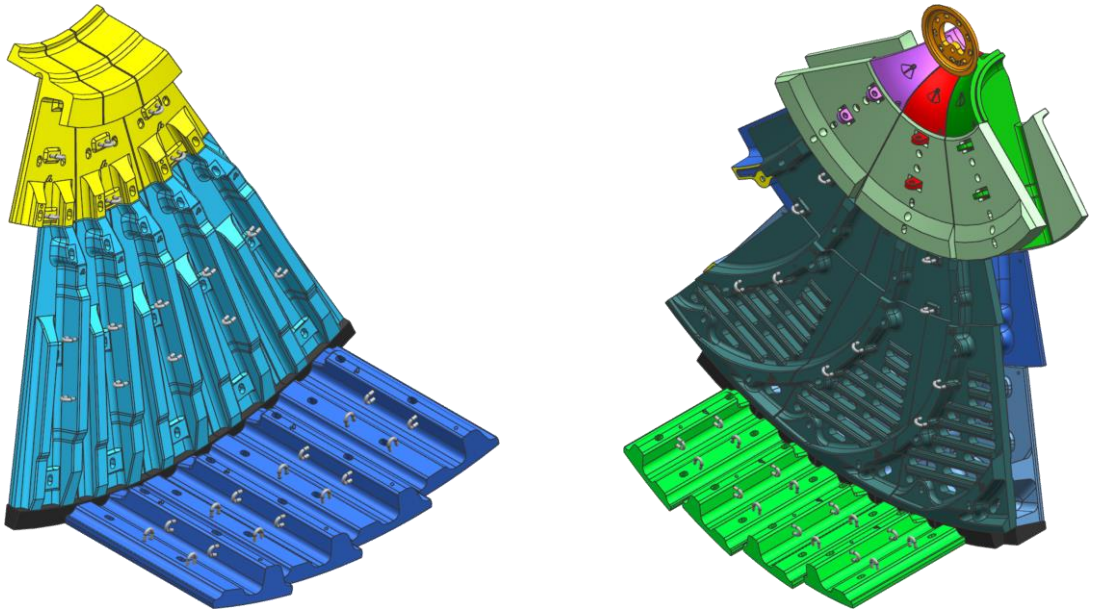

Figure 8: General Assembly of Final Revisions

The final design included:

- Half-row double wide Vortex discharge system
- Revised Vortex grates with 3.75in slots and 534in^2 open area.
- Two trial high-chrome Vortex grates for validation.
- Revised uni-directional shell liners with 15° leading face angle to promote prolonged attrition grinding.

PERFORMANCE GUARANTEE AND FORECAST MODEL

Through Bradken's continued optimisation process, enough data was gathered to provide the framework for a guaranteed performance improvement. The agreement required site to share the following metrics bi-weekly on a per minute basis for performance tracking:

- Fresh feed – tph
- Recycling feed – tph
- Water feed – tph
- Power draw – kW
- Mill bearing pressure – kPa
- f80 – mm
- f50 – mm

As well as the following geo-metallurgical data collected on a daily basis:

- Rock quality designation (RQD) – %
- Bond work index (BWi) – kwh/t
- Ore density – t/m^3

In addition to monitoring these parameters for the performance guarantee, Bradken devised a machine learning based mill throughput prediction model to verify results and forecast future performance.

Performance Guarantee Summary

The initial study of the time series trend of data suggested that the water feed and recycle feed exhibited similar moving trends with the throughput results. The ore properties showed some correlation to throughput results. The mill bearing pressure showed a strong correlation to power draw. The statistics of the datasets are shown in **Table 2**.

Table 2: Statistics of Collected AG Mill Dataset and from DEM Modelling

Variable	Statistics			
	Min	Max	Mean	Standard
Bearing Pressure – kPa	482.19	690.36	646.30	33.48
F80 – mm	66.88	123.12	101.89	14.44
Water Feed – t/h	228.78	1629.24	1172.16	196.03
Recycle Rate – t/h	76.83	936.38	498.31	109.08
Throughput – t/h	175.02	1074.44	819.38	132.16
RQD – %	18.75	58.21	34.92	9.73
BWi – kWh/t	12.39	15.66	14.25	0.51
Rock Density – t/m^3	2.57	2.72	2.61	0.11
Total Normal (Impact) Collisional Energy - kJ	12.36	207.03	162.12	10.35
Total Tangential (Abrasion) Collisional Energy - kJ	174.68	529.25	371.89	21.17
Total Open Area – m^2	8.03	11.16	9.44	1.13

The average throughput was defined as the measured feed rate trimmed to remove the non-operational portion. The results exceeded the performance guarantee with an average performance of 891.4tph.

Mill Throughput Model Development

The decision tree-based ensemble method was selected for model development as it was highly suited for mill throughput prediction. It offered the most model flexibility, low over-fitting and high computation efficiency; as well as, feature importance ranking capability.

Ensemble learning integrates multiple learning algorithm to obtain improved predictive results than using any of the single algorithm alone (T. G. Dietterich, 2002). Bagging, boosting and stacking are the three main categories of ensemble learning methods, and the boosting method is mostly commonly used. The boosting method continuously iterates and constructs evaluators for predictions, so each evaluator is inter-correlated, and the prediction result is determined by weighting and summing the results. The representative model of the boosting includes Adaboost (A. Shahraki, 2020) and gradient boosting tree (C. Bentéjac, A. Csörgő, and G. Martínez-Muñoz, 2021). The extreme gradient boosting (XGBoost) algorithm (T. Chen et al., 2015) is an improved method developed based on the gradient boosting method.

Predictive performance of XGBoost is based on a prediction score generated on each leaf node, and it is treated as the regression value of all samples on this leaf. Such prediction score is named as leaf weight, which is expressed as $f_k(x_i)$. Therefore, the overall regression result of the ensemble model is the sum of predicted scores on all trees, and prediction result of the model on i-th sample is,

$$\hat{y}_i^{(k)} = \sum_k^K f_k\,(x_i) \tag{1}$$

where f_k represents the *k*-th decision tree, and x_i represents the feature vector corresponding to sample *i*. Hence, the objective function of XGBoost is then,

$$Obj = \sum_{i=1}^{m} l\,(y_i, \hat{y}_i) + \sum_{k=1}^{K} \Omega\,(f_k) \tag{2}$$

where, *m* represents the total amount of data imported into the *k*-th tree.

The objective function above is simplified by iteration and Taylor expansion, and the sample *i* in the objective function is reduced to each leaf *j* for solution, and the objective function on the *t*-th tree is finally obtained as:

$$Obj^{(t)} = -\frac{1}{2}\sum_{j=1}^{T}\frac{G_j^2}{H_j+\lambda} + \gamma T \quad (3)$$

where

- the number of leaf nodes contained in the t-th tree is T,
- j is the leaf node index, $G_j = \sum_{i\in I_j} g_i$, and $H_j = \sum_{i\in I_j} h_i$; g_i and h_i are the first derivative and the second derivative of the $\hat{y}_i^{t-1}$ obtained on the loss function $l\left(y_i^t,\ \hat{y}_i^{t-1}\right)$, respectively.

$$\text{Gain} = \frac{1}{2}\left[\frac{G_L^2}{H_L+\lambda} + \frac{G_R^2}{H_R+\lambda} - \frac{(G_L+G_R)^2}{H_L+H_R+\lambda}\right] - \gamma \quad (4)$$

where, *L* and *R* represent the left and the right side of the binary trees, respectively.

XGBoost algorithm features high accuracy and flexibility, lower degree of overfitting, and is easier to compensate missing value and parallel computation. Nevertheless, XGBoost algorithm also performs repetitive indexing of all data for calculation of the information gain; and hence, this method generally requires larger memory, especially when processing high dimension or large amount of data. Therefore, the efficiency and scalability challenges of the XGBoost algorithm are prominent.

Data Curation

The mutual information method was initially utilized to investigate the level of correlation between each variable and the predicting metric. Compared with the F-test method, the mutual information method can find any relationship between features and predictors, including linear and nonlinear correlations (H. Casini, M. Huerta, R. C. Myers, and A. Yale, 2015). Error! Reference source not found. shows the estimated values of mutual information between each characteristic variable and the throughput. It was indicated that all characteristic variables are correlated to the throughput, with RQD exhibited largest correlation, and F80 exhibited least correlation.

Table 3: Mutual Information Estimated Value Between Each Characteristic Variable and the Throughput

Parameter	Mutual Information	Parameter	Mutual Information
Water Feed	0.454	BWi	0.447
Recycle Feed	0.158	Rock Density	0.430
Bearing Pressure	0.189	RQD	0.469
F80	0.106	Total Normal Collisional Energy	0.254
Total Open Area	0.413	Total Tangential Collisional Energy	0.426

Model Training

The entire dataset was segmented into two groups, training, and validation. To improve the model training, 85% of the entire dataset was configured as training, and 15% was used for validation.

Cross-validation is a commonly used method for machine learning modelling and parameter verification. The K-fold cross-validation method was adopted in this study (T.-T. Wong and P.-Y. Yeh, 2019). Essentially, the original data was segmented into K groups, and a test set was constructed for each subset. The remaining K-1 subsets were then used as training sets. By this means, a total of K models and K model prediction scores are obtained. K-fold cross-validation can effectively avoid over-fitting and under-fitting. In this study, K was selected as 10 to obtain 10 sets of training models and evaluation scores. Here we use R^2, and root mean square error (RMSE) to measure the effect of the learning model.

$$R^2 = 1 - \frac{\sum_{i=0}^{m}(y_i - \hat{y}_i)^2}{\sum_{i=0}^{m}(y_i - \bar{y})^2} = 1 - \frac{RSS}{\sum_{i=0}^{m}(y_i - \bar{y})^2} \quad (5)$$

$$MSE = \frac{1}{N}\sum_{t=1}^{N}(y_t - \hat{y}_t^2) \quad (6)$$

$$RMSE = \sqrt{\frac{1}{N}\sum_{t=1}^{N}(y_t - \hat{y}_t^2)} \quad (7)$$

where,

- y_i is the true label,
- $\hat{y}_i$ is the predicted result,
- $\bar{y}$ is the mean,
- and N is the number of samples.

XGBoost is an ensemble algorithm based on the improvement of the gradient boosting tree, which is comprised of ensemble algorithm itself, the weak estimator, and other associated calculation processes. Similar to other decision trees and tree integration methods, XGBoost model features multiple hyperparameters, including the number of ensemble weak evaluators, the maximum depth of each tree in the weak evaluator, and the regularization parameters λ and γ.

In order to facilitate the selection of the optimal hyperparameter combination, R^2 and RMSE were used as evaluation indicators to optimize the hyperparameters using a combination of grid searching and cross-validation. **Error! Reference source not found.** shows selected XGBoost hyperparameters that need to be optimized and their corresponding grid search range. Readers are directed to the Appendix for detailed parameter definitions.

Table 4: Prediction Model Hyperparameters and Grid Search Range

XGBoost Hyperparameter	Grid Search, Range (Min, Max, Step)
N_estimators	100, 1000, 20
subsample	0, 1, 20
max_depth	1, 20, 20

eta	0.01, 1, 50
gamma	0, 50, 50
lambda	0, 50, 20
alpha	0, 50, 20
colsample_by tree	0, 1, 10
colsample_by level	0, 1, 10
colsample_by node	0, 1, 10

Utilizing model hyperparameters shown in **Table 4** for cross-validation, predictive performance of XGBoost model on test datasets was obtained. As shown in **Table 5**, XGBoost model already offers relatively high levels of predictive accuracy using the default hyperparameters, further improvement is to be obtained after the model optimization process discussed below.

Table 5: Initial Predictive Performance Results for the XGBoost Model

Variable	Model Performance R^2	RMSE
R^2 Max	0.8139	69.37
$RMSE_{min}$	0.7981	65.01

Hyperparameter Optimisation

In order to further improve the model accuracy, reduce overfitting and enhance model generalization, it is essential to optimize the hyperparameter settings. This is performed by alternating the hyperparameter combinations as listed in **Table 4**. Resulting R^2 scores or RMSE scores from current and new hyperparameter settings are compared to determine if any improvements have been achieved. **Figure 9** shows that both R^2 score and RMSE score converged with increasing number of estimators using hyperparameters in **Table 4**. It was indicated that the R^2 score converged quicker than the RMSE score with a smaller number of estimators. Therefore, the following hyperparameter optimization process evaluation was based on the RMSE score below.

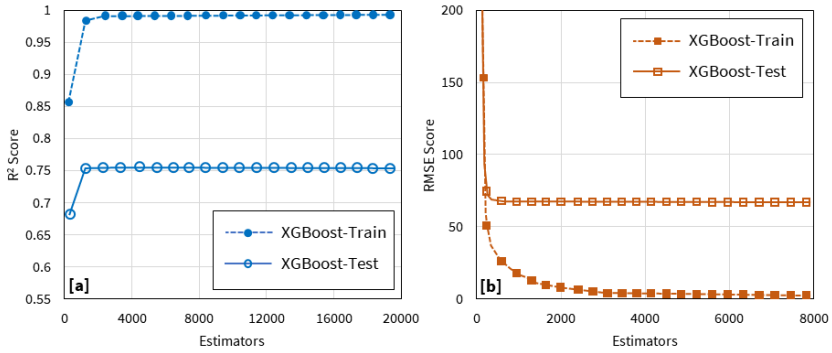

Figure 9: Cross-Validation Learning Curves of the Current Hyperparameter Setting Based on R^2 Score and RMSE Score

The principle of the hyperparameters optimization was set as:

- RMSE score difference between the training set and the test set should be reduced with the new hyperparameter setting,
- The RMSE score of the test set with the new hyperparameter setting should be decreased.

By applying the above method and looping through the hyperparameter settings, the optimal hyperparameter combinations for both XGBoost was obtained. As shown in **Figure 10** for the cross-validation curve of the XGBoost model, overfitting level has been greatly reduced compared with the original hyperparameter settings. Final RMSE score for the test set of optimized XGBoost model was observed to be around 67.

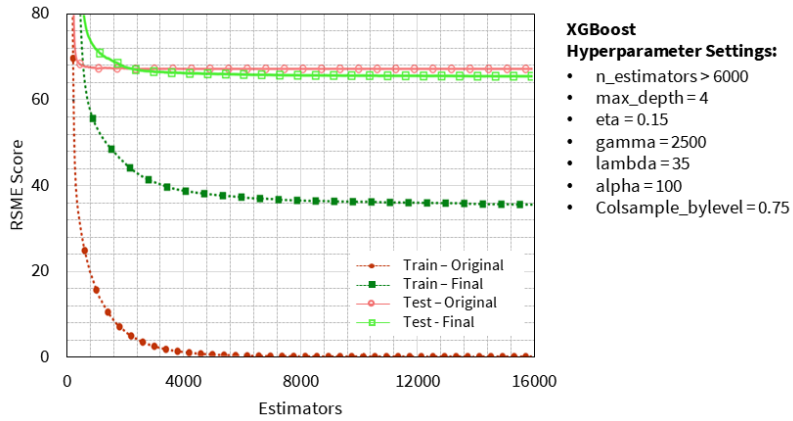

Figure 10: Comparison Between the Original and Optimised Cross-Validation Curves for the XGBoost Model

Ensemble Model Predictive Performance

Once the XGBoost model completed training with hyperparameters selection using the initial 85% of the datasets, the model was tested against the validation dataset. Predictive results of the trained XGBoost model with the input parameters were obtained and compared with the validation dataset, and results are shown in **Figure 11**. It was observed that the XGBoost model predictions closely matched the moving trend of the validation dataset. However, there was a sudden reduction in the throughput observed, higher deviations between the predictive results and validation dataset were observed.

The overall predictive performance of the trained XGBoost model on the validation dataset is shown in **Error! Reference source not found.**. Compared with the classic geo-metallurgical theory-based predictions (S. Morrell, 2004), the method employed in this study showed improvements in both the qualitative trend and quantitative accuracy (B. Burger, K. McCaffery, I. McGaffin, A. Jankovic, W. Valery, and D. La Rosa, 2006).

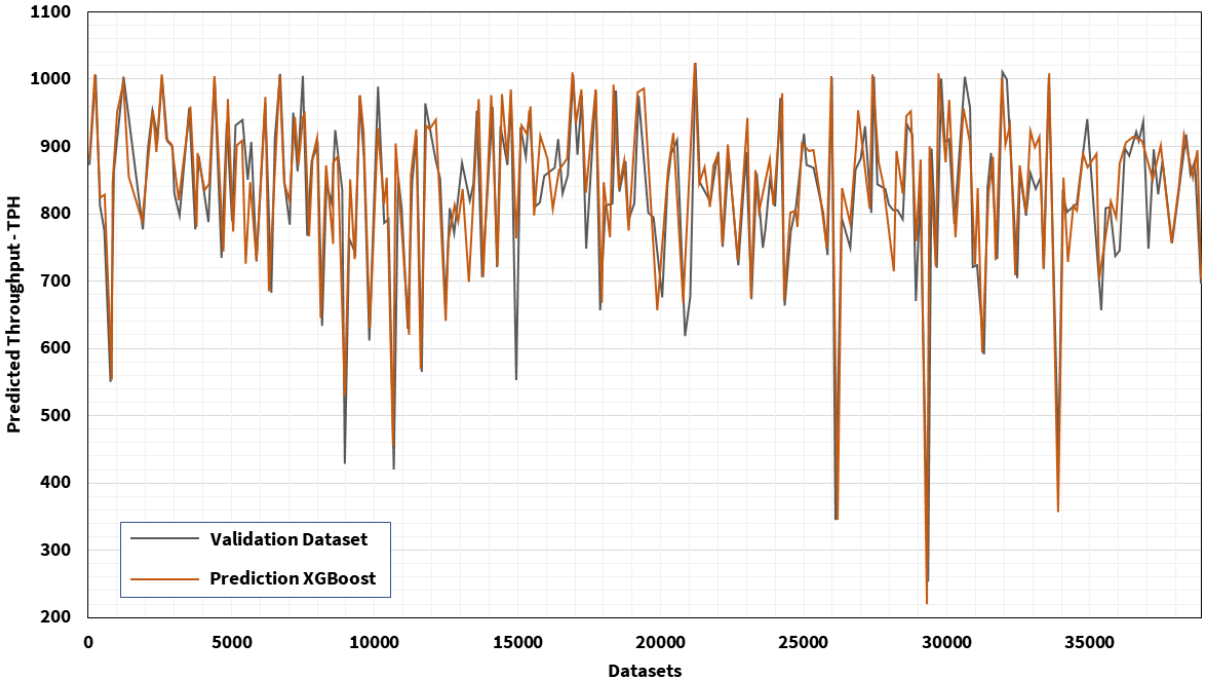

Figure 11: Comparison Between XGBoost Model Predictions and the Validation Dataset

Pearson Correlation on Predictive Performance

Pearson's correlation analysis (J. Benesty, J. Chen, Y. Huang, and I. Cohen, 2009) was additionally performed on the predictive performance to evaluate its the statistical significance. The Pearson correlation coefficient r is defined as:

$$r = \frac{\sum_{t=1}^{N}(y_t-\bar{y})(\hat{y}_t-\bar{\hat{y}})}{\sqrt{\sum_{t=1}^{N}(y_t-\bar{y})^2\sqrt{\sum_{t=1}^{N}(\hat{y}_t-\bar{\hat{y}})^2}}} \quad (8)$$

The probability density function of the Pearson correlation coefficient r is defined as:

$$f(r) = \frac{(1-r^2)^{\frac{N}{2}-2}}{B\left(\frac{1}{2},\frac{N}{2}-1\right)} \quad (9)$$

where,

- N is the sample quantity,
- $\bar{\hat{y}}$ is the average prediction result
- B is the Beta function.

Results of the Pearson correlation analysis of the prediction performance are shown in **Figure 12**. The Pearson correlation coefficients between the predicted and validation dataset for the trained model is over 0.92. Additionally, the significant level is lower than the 5% threshold. Such result indicated that XGBoost trained model exhibited high reliability and generalization capability.

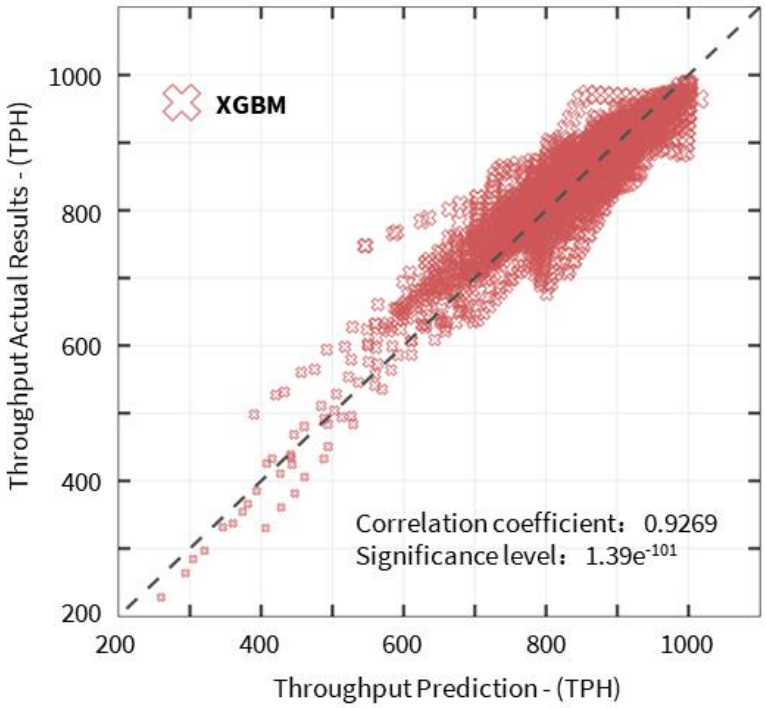

Figure 12: Pearson' Correlation for Developed XGBoost Model Predictions

Feature Importance Analysis

Based on aforementioned comments, each studied mill operating parameter induces varied impacts on the mill's throughput performance. XGBoost method offers the capability to quantify the feature importance for selected parameter. There are three methods for modelling the feature importance for XGBoost models, namely, weight, gain and cover. Weight is the total number of times that each feature appears in the model prediction or is used as a branch node; gain calculates the average information gain after a specific feature is used for the branch; cover represents the average number of all samples processed in each branch for a specific feature. In this study, the gain metric was selected to model the feature importance for studied parameters.

The feature importance for each studied parameter was estimated by the gain metric and results are shown in **Figure 13**. Feed water was observed to exhibit highest gain percentage, followed by Total Tangential Collisional Energy, Total Open Area, Recycle Feed, Bearing Pressure, Total Normal Collisional Energy, F80, BWi, Ore Density, F50 and RQD. This result suggested that Water Feed showed most dominant impact on the mill's throughput performance. This observation differs from the conventional grind curve approach which assigns less importance to the feed water. This may be due to the fact that the product stream generated by the grinding dynamics requires sufficient water feed to transport the product out of the mill. Liner wear (total collisional energy and open area) also exhibited relatively higher impact on the throughput compared with the ore properties.

The above analysis has practical significance on mill operations. Appropriate level of the feed water is required to ensure that product discharge is achieved efficiently at maximum throughput. Additionally, optimal liner profile is required to maintain the total collisional energy at high level for the ore of specific properties.

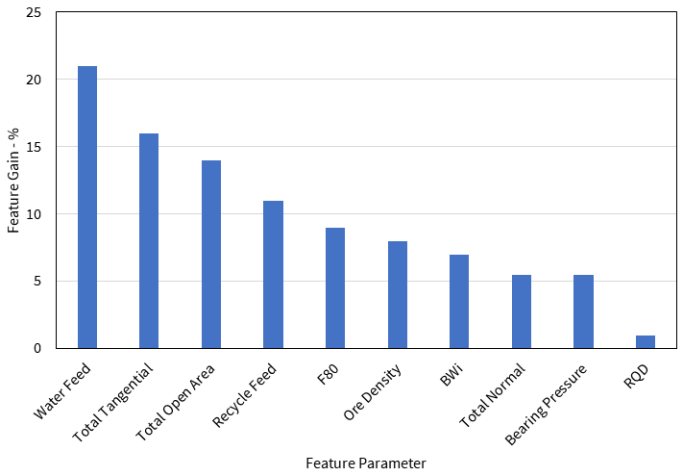

Figure 13: Feature Importance Ranking Results based On Feature Gain in Developed XGBoost Model

Conclusions

Through the installation of Bradken's liner package, and a continued development and collaborative approach, the performance objectives of the partner site were achieved. The shell liners were optimised using DEM-based collision energy with results from various configurations of worn shell liner reviewed against monitored wear performance to identify peak performance periods during service life. The discharge capacity was achieved by implementing a half-row double wide Vortex discharge end design, including optimised slot placement as developed based on DEM-SPH numerical modelling framework.

The total liner package exceeded the performance guarantee producing an average throughput of 891.4tph and improved achieved 9.5% more than the previous per-Bradken liner set; as well as, a reduction in mill specific energy of 2.5%. The two high-chrome grates achieved the target wear life of 210 days in service and milled 3.76Mt validating the design for full supply.

The throughput performance of the AG mill was successfully predicted using an ensemble learning method. The developed XGBoost machine learning model was successfully correlated to the validation dataset. The developed XGBoost model also showed high reliability and generalization capability. Feature importance in the XGBoost model was also studied and results suggested that the water feed and liner wear exhibited higher impact on the mill's throughput performance, followed by ore properties. This developed methodology has a potential to improve production planning process involving AG mill in the mineral processing circuit.

FURTHER STUDY

As a point of further study, Bradken is exploring developing a recycle rate prediction model to forecast potential downstream impacts of increased throughput performance.

References

T. G. Dietterich (2002), “Ensemble learning,” Handb. brain theory neural networks, vol. 2, no. 1, pp. 110–125.

A. Shahraki (2020), M. Abbasi, and Ø. Haugen, “Boosting algorithms for network intrusion detection: A comparative evaluation of Real AdaBoost, Gentle AdaBoost and Modest AdaBoost,” Eng. Appl. Artif. Intell., vol. 94, p. 103770.

C. Bentéjac, A. Csörgő, and G. Martínez-Muñoz (2021), “A comparative analysis of gradient boosting algorithms,” Artif. Intell. Rev., vol. 54, no. 3, pp. 1937–1967.

T. Chen et al. (2015), “Xgboost: extreme gradient boosting,” R Packag. version 0.4-2, vol. 1, no. 4, pp. 1–4.

H. Casini, M. Huerta, R. C. Myers, and A. Yale (2015), “Mutual information and the F-theorem,” J. High Energy Phys., vol. 2015, no. 10, pp. 1–70.

T.-T. Wong and P.-Y. Yeh (2019), “Reliable accuracy estimates from k-fold cross validation,” IEEE Trans. Knowl. Data Eng., vol. 32, no. 8, pp. 1586–1594.

S. Morrell (2004), “Predicting the specific energy of autogenous and semi-autogenous mills from small diameter drill core samples,” Miner. Eng., vol. 17, no. 3, pp. 447–451, doi: 10.1016/j.mineng.2003.10.019.

B. Burger, K. McCaffery, I. McGaffin, A. Jankovic, W. Valery, and D. La Rosa (2006), “Batu Hijau model for throughput forecast, mining and milling optimization, and expansion studies,” 2006 SME Annu. Conf. - Adv. Comminution, vol. 2006, no. March 2017, pp. 461–479.

J. Benesty, J. Chen, Y. Huang, and I. Cohen (2009), “Pearson correlation coefficient,” in Noise reduction in speech processing, Springer, pp. 1–4.

Copyright Form for SAG 2023

Title of Paper: _____

_____

_____

Author(s): _____

_____

GRANTING OF COPYRIGHT

I/WE HEREBY AGREE TO GRANT THE RIGHT TO PUBLISH MY/OUR PAPER BOTH IN CONFERENCE PROCEEDINGS AND IN ON-LINE LIBRARIES TO THE SAG CONFERENCE FOUNDATION, WHEN THE PAPER IS ACCEPTED FOR PUBLICATION IN THE SAG 2023 PROCEEDINGS. I/WE CERTIFY THAT THE CONTENTS OF THIS PAPER HAVE NOT BEEN COPYRIGHTED, PUBLISHED, OR SUBMITTED FOR PUBLICATION ELSEWHERE.

Author(s)'s Signature(s)

Date _____

Name(s) (please print) _____

If this paper represents work made for hire:
Name and title of the person for
whom work was done (please print) _____

_____

Authorizing signature: _____

IF YOU SUBSEQUENTLY SUBMIT YOUR PAPER TO ANOTHER PUBLICATION, PLEASE BE SURE TO INDICATE THAT THE PAPER WAS FIRST PUBLISHED IN THE SAG 2023 PROCEEDINGS, CITING LOCATION AND DATE.

IF YOUR PAPER, OR SUBSTANTIAL PARTS OF IT, HAVE BEEN PUBLISHED ELSEWHERE AND ARE ALREADY UNDER COPYRIGHT TO ANOTHER ENTITY, THEN IT IS YOUR OBLIGATION TO ENSURE THAT THE SAG CONFERENCE FOUNDATION CAN PUBLISH THIS WORK.